

High-Resolution Photoemission Study of the Band Structure of Tellurium

L. D. Laude, B. Fitton, and M. Anderegg

Surface Physics Division, European Space Research Organization, Noordwijk, Holland

(Received 16 November 1970)

Second-derivative spectra of photoelectron energy distributions from vacuum-cleaved Te were obtained with polarized light of energy 5.2 to 9 eV. Resolution was between 50 and 100 meV using modulation amplitudes up to 1.0 V. Five main structures arise as a result of transitions from the p -valence-band triplets, in good agreement with band-structure calculations. For the first time d -conduction-band minima can be located unambiguously at 5.0, 5.6, and 6.3 eV above the valence-band edge.

Tellurium band-structure calculations¹⁻⁴ have largely been concerned with the features of the two p valence bands and the p -like conduction band originating from the $5s^25p^4$ atomic configuration, each of these bands being a triplet because of the presence of three atoms in the unit cell. These calculations show appreciable differences, but they tend to confirm the presence of an energy-gap minimum about the H point, in agreement with experiment, and rather flat valence bands along the Δ and S directions with sub-band splittings of the order of 100 meV. In this study we have for the first time been able to determine directly the position of these two p valence bands, and in addition to locate minima in the d conduction band. No information could be obtained on the p conduction band since this lies well below the vacuum level.

Optical measurements provide only the transition energies; and because of the added complication of large changes in oscillator strength through k space in tellurium,⁵ it has not been possible to provide definite assignments for the higher energy peaks in the optical spectrum.^{6,7} Photoemission energy-distribution curves (EDC's), obtained from the first derivative of the photocurrent,⁸ have the distinct advantage that, when observed over an extended range of excitation energies, the characteristics of the peaks can identify initial and final states of the transitions and relate their energy positions to the vacuum level.⁹ The use of polarized light in this work reduced further uncertainties in these assignments. It was apparent, however, that a high-resolution method of determining the energy distribution of photoelectrons was required in view of the narrowness of the p bands and their triplet nature.^{10,11} These determinations were therefore made using a gold-coated spherical collector and synchronously detecting the third harmonic of the ac modulation applied to the retarding ramp voltage in order to obtain the third derivative of

the photocurrent.^{12,13}

The third derivative is proportional to the amplitude of the third harmonic only for small values of the modulation amplitude A , larger amplitudes introducing distortion due to the inclusion of higher odd-derivative terms.¹⁴ If, for example, a Gaussian form with a full width σ at half-maximum is used for the photoemission spectrum, then significant distortion is present for $A \geq \sigma$. However, since this distortion is due to higher odd derivatives, the zero-crossing points and position of the center of the peak of the derivative are not seriously affected, and the energy resolution can be maintained to large modulation amplitudes with a consequent gain in signal-to-noise ratio.¹⁵ Although this method is of general use, it has proved particularly advantageous in this study where the requirement of high resolution over an extended wavelength range, including polarization requirements, posed serious problems in signal-to-noise ratios even with repetitive scanning and storage in a signal averager.

Figure 1 illustrates the resolution, of the order of 100 meV, obtainable using a modulation amplitude of 1 V peak to peak. The normal EDC's, obtained with a 0.3-V peak-to-peak modulation, are shown for comparison and labeled (a) and (b) according to the polarization. Three structures can be distinguished. In the third derivative (c), the peaks (2) and (2') are quite clearly separated. As no structure exists on the low-energy side of the main peak (1), then, with the assumption of the symmetry of a Gaussian distribution for the corresponding structure in first-derivative spectra, the right half is considered to be a reflection through the vertical axis of (1). With the same approximation in the case of the minor high-energy peak (2'), the shape of peak (2) can be resolved which then allows the main peak (1) to be corrected for the negative section of (2) as illustrated.

A comprehensive survey of these measure-

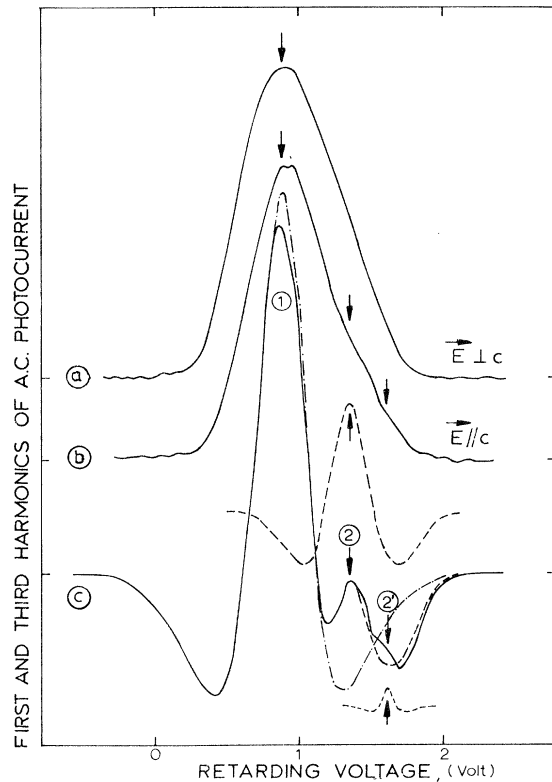


FIG. 1. Photoemission spectrum of a Te $(10\bar{1}0)$ face, at $h\nu = 6.36$ eV. Curves (a) and (b) show the EDC's for light polarized parallel and perpendicular to c axis, respectively. In (c) is shown the third harmonic of the photocurrent for nonpolarized light, (1), (2), and (2') referring to structures defined in the text. Note on (b) the two small structures appearing on the high-energy side and not resolved in (a). These two structures are clearly resolved in (c).

ments on the $(10\bar{1}0)$ face of tellurium, cleaved in 10^{-11} Torr, is given in Fig. 2. This shows the behavior of the main detected structures as a function of photon energy (5.2–9.0 eV) used for exciting electrons from the valence-band triplets. Despite their differences, the available band-structure calculations agree on two points:

(1) The s band lies about 8 eV below the top of the valence band, and (2) the width of the p -conduction-band triplet does not exceed 2 eV. Considering that the vacuum level as determined in this work lies at 4.65 ± 0.05 eV above the valence-band edge, it is expected that none of the electrons excited either directly or indirectly (via electron-phonon interaction) to the p conduction band (p_3) could be emitted into vacuum; therefore none of the observed structures could be attributed to $s \rightarrow p_3$ transitions. Furthermore, in the spectral range used in this work no $s \rightarrow d$ transitions are possible since they will require

excitation energies of the order of 12 or 13 eV. Consequently the measured photoemission spectra, which were precisely followed from 5.2 to 9 eV, can be interpreted in terms of direct or indirect transitions between the p -valence-band triplets and the d -band levels above the vacuum level. The only structure which cannot be fitted into that scheme is structure (1*) which appears at $h\nu \approx 7.5$ eV and remains stable at $\mathcal{E} \approx 4.9$ eV, increasing rapidly in strength with photon energy. This structure is therefore assumed to result from scattering processes in the crystal.¹⁶

The first structures appearing at low energy [(1), (2), (2'), and (3)] close to the photoelectric threshold were resolved with a 50-meV accuracy using 0.4- to 0.5-V modulation amplitudes. They can be assigned to transitions originating from the p_2 upper valence-band triplet. Indirect processes involving the relaxation of electrons¹⁷ are responsible for (1) which remains stationary with increasing photon energy, indicating a d -band minimum 5.0 eV above the valence-band edge. This structure, (1), weakens quickly and ultimately disappears around $h\nu = 7.1$ eV. The structures (2) and (2') are localized 0.7 and 0.3 eV, respectively, below the valence-band edge, corresponding to two structures in the p_2 -valence-band density of states localized at these energies. Furthermore, (2) and (2') behave like doublets in the low-energy part of the spectrum (much smaller width and doublet resolved at low energy). This doublet structure can only be due to the p_2 degeneracy about the critical points; and (2), together with (2'), is likely to be due to transitions initiated at (or close to) one or more of these points.

Structure (3) is localized about 1.5 eV below the valence-band edge. According to Treusch and Sandrock's Korringa-Kohn-Rostoker band calculations,² this would indicate that the transitions originate from the lowest p -valence-band triplet. However pseudopotential calculations give bandwidths about 1 eV larger¹⁴ and provide a better fit to other experimental features than the former calculation. This being the case, structure (3) is likely to be due to a further set of transitions from the p_2 -valence-band levels. A strong polarization effect is also observed on (3) as shown in Fig. 3, which emphasizes its triplet behavior between 7.3 and 8.1 eV. This region of structure (3) can therefore be attributed to transitions from points along Δ or P of p_2 where selection rules make such a segregation possible.

Structure (4) appears about $h\nu \approx 7.0$ eV and

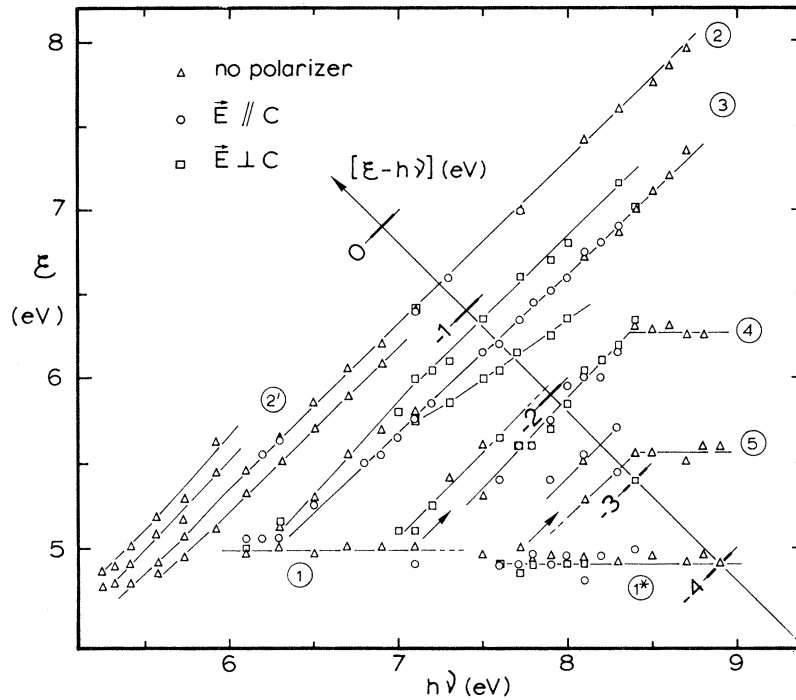


FIG. 2. Energy diagram of the different structures appearing in the photocurrent third harmonic. Obtained from a Te ($10\bar{1}0$) face as a function of photon energy $h\nu$ in the range 5.2–9.0 eV for light polarized parallel or perpendicular to c axis. Nonpolarized light data are quoted when necessary to localize structures not sufficiently resolved with polarized light. Final photoelectron energies (\mathcal{E}) relative to the top of the valence band are on ordinate, and excitation energies ($h\nu$) on abscissa. Localization of structures in the valence-band density of states can be obtained by direct reading on the axis across the diagram, on which initial electron energies ($\mathcal{E}-h\nu$) are quoted.

remains stationary in the valence band at around -2.0 eV, below the valence-band edge. This probably corresponds to transitions arising from

the top of the p_2 band. These transitions undergo an indirect process¹⁷ towards a d -band minimum starting near $h\nu \approx 8.4$ eV, as indicated by a stationary structure located 6.3 eV above the valence-band edge. Finally, structure (5), centered at -3.0 eV, could be attributed to transitions initiated at the bottom of the p_1 band, in agreement with pseudopotential band-structure calculations.⁴ This structure also evolves, around $h\nu \approx 8.4$ eV, into a stationary structure at $\mathcal{E} = 5.6$ eV, localizing another d -band minimum¹⁷ between the two other conduction-band levels positioned by (1) and (4).

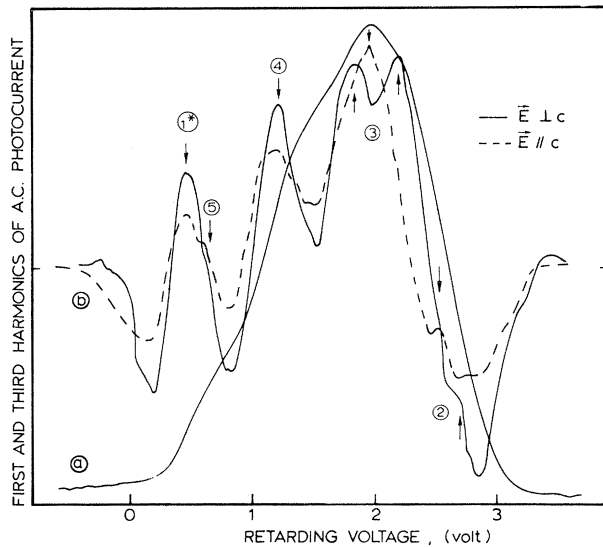


FIG. 3. Energy distribution curve (a) and third harmonic of the photocurrent (b) obtained from a Te ($10\bar{1}0$) face for $h\nu = 7.72$ eV and light polarized perpendicular to c -axis.

Additional features of the d conduction band, and also the location of the s valence band, will require higher excitation energies for their investigation. An extension of these studies is therefore being undertaken using photon energies up to 21 eV.

The authors thank Dr. E. A. Trendelenburg, Dr. B. Feuerbacher, and Dr. R. F. Willis of the European Space Research Organization, and Dr. U. Rössler of Marburg University for very helpful discussions, and M. Barnes for his enthusiastic and very competent assistance.

- ¹R. E. Beissner, *Phys. Rev.* **145**, 479 (1966).
²J. Treusch and R. Sandrock, *Phys. Status Solidi* **16**, 487 (1966).
³H. G. Junginger, *Solid State Commun.* **5**, 509 (1967).
⁴M. Hulin and M. Picard, *Solid State Commun.* **7**, 1587 (1969); T. Doi, K. Nakao, and H. Kamimura, *J. Phys. Soc. Jap.* **28**, 36 (1970).
⁵R. Sandrock, *Phys. Rev.* **169**, 642 (1968).
⁶J. D. Hayes, E. T. Arakawa, and M. W. Williams, *J. Appl. Phys.* **39**, 5527 (1968).
⁷S. Tutihasi, G. G. Roberts, R. C. Keezer, and R. E. Drews, *Phys. Rev.* **177**, 1143 (1969).
⁸W. E. Spicer and C. N. Berglund, *Rev. Sci. Instrum.* **35**, 1665 (1964).
⁹N. V. Smith and W. E. Spicer, *Opt. Commun.* **1**, 157 (1969); T. E. Fischer, *Surface Sci.* **13**, 30 (1969).
¹⁰B. Kramer and P. Thomas, *Phys. Status Solidi* **26**, 151 (1968).
¹¹H. Merdy, *Ann. Phys. (Paris)* **1**, 289 (1966).
¹²N. V. Smith and M. M. Traum, *Phys. Rev. Lett.* **25**, 1017 (1970).
¹³L. W. James, R. C. Eden, J. L. Moll, and W. E. Spicer, *Phys. Rev.* **174**, 909 (1968).
¹⁴N. J. Taylor, *Rev. Sci. Instrum.* **40**, 792 (1969).
¹⁵J. H. Beynon, S. Clough, and A. E. Williams, *J. Sci. Instrum.* **35**, 164 (1958).
¹⁶C. N. Berglund and W. E. Spicer, *Phys. Rev.* **136**, A1030, A1044 (1964).
¹⁷L. W. James and J. L. Moll, *Phys. Rev.* **183**, 740 (1969).

Experimental Evidence of Two-Electron Transitions in Solids*

K. Betzler and T. Weller

Physikalisches Institut der Universität Stuttgart, D-7000 Stuttgart, Germany

(Received 9 February 1971)

A new emission band at $h\nu = 2E_g$ is observed in Si using carrier injection in a p - n device. The extremely weak photon emission was detected by a special differential counting technique. From the photon energy, the quadratic dependence on the excitation intensity, and the weak temperature dependence, it is concluded that the observed emission is caused by a two-electron transition.

Two-electron transitions have been known for a long time in atomic physics as autoionization spectra. Heisenberg¹ has pointed out the selection rules for these transitions, $\Delta l_1 = \pm 1$ and $\Delta l_2 = 0, \pm 2$. In contrast to the situations in atoms, in solids it should be possible for both electrons to have the same initial state and the same final state. In the octahedral rotation group O , for example, two-electron transitions should be allowed from the Γ_4 or Γ_5 level to the Γ_1 , Γ_2 , Γ_3 , Γ_4 , or Γ_5 level.

To avoid frequency doubling of the one-electron transition by nonlinear optical effects, a crystal with inversion symmetry should be used. In this case two-electron transitions are forbidden because of the parity selection rule. In the space group, this selection rule does not hold. Therefore a crystal should be used in which at least one of the band extrema, i.e., the valence-band maximum or the conduction-band minimum, does not lie at the Γ point. In Si, which has O_h symmetry, the conduction-band minimum lies near the X point and the valence-band maximum is a Γ_5^+ state.² The different positions of these extrema in k space produces a weak one-electron transition because of momentum conservation, while the two-electron transition is permitted.

An additional advantage of this substance is the fact that it can easily be excited by injection when used as a p - n junction device.³ In absorption this effect cannot be observed because of the strong one-electron absorption at the energy $h\nu = 2E_g$.

Minority carriers in Si were generated in a cylinder of about 0.2 mm length and 0.2 mm diam by means of a forward-biased p - n junction. The recombination outside the junction region was investigated. Two types of diodes are investigated, with n - and with p -type bulk material. The resistivity of the bulk material was of the order of 1 Ω cm. Since the injection-current densities were very high (of the order of 10^4 A cm⁻²), experiments were performed with pulses of 22 μ sec length and at a duty cycle of 1%. The electric fields in the bulk region of the sample were less than 10^2 V cm⁻¹. The samples were mounted on a copper heat sink, whose temperature was controlled. From thermal conductivity data a temperature difference of less than 10°K between sample and heat sink was estimated.

The following experimental system was used to detect an extremely weak radiation at about twice the energy gap of Si (i.e., at a wavelength near 5600 Å). For registration of the signal, a